Investigation of the fluxes to a surface at grazing angles of incidence in the tokamak boundary

1990 Plasma Phys. Control. Fusion 32 1301

(http://iopscience.iop.org/0741-3335/32/14/004)

Plasma Physics and Controlled Fusion, Vol. 32, No. 14, pp. 1301 to 1320, 1990
Printed in Great Britain.

0741-3335/90 $3.00 + .00
IOP Publishing Ltd. and Pergamon Press plc

INVESTIGATION OF THE FLUXES TO A SURFACE AT GRAZING ANGLES OF INCIDENCE IN THE TOKAMAK BOUNDARY

G. F. MATTHEWS, S. J. FIELDING, G. M. MCCRACKEN, C. S. PITCHER,*‡
P. C. STANGEBY† and M. ULRICKSON‡
Culham Laboratory, UKAEA/Euratom Fusion Association, Abingdon, Oxon OX14 3DB, U.K.

(*Received* 5 *March* 1990; *and in revised form* 28 *August* 1990)

Abstract—This paper describes an experimental investigation of the effects of grazing angles of incidence on the fluxes of power and particles to a surface inserted into the boundary of the DITE Tokamak. Related thermographic data from the TFTR Tokamak are also presented. A summary is given of the important issues relating to angle of incidence which are relevant to large Tokamaks such as JET, NET and ITER and which require experimental confirmation. An array of Langmuir probes has been constructed to carry out experiments as a function of angle on DITE. Results from this Tilting Probe Array (TPA) are described, which show how the ion saturation current, electron saturation current, floating potential and the fitted electron temperature vary with surface angle. It is shown that when the magnetic field is at grazing angles of incidence to the surface a conventional interpretation of the probe characteristics fails completely. Power flux distributions from infra-red thermography of the TFTR moveable limiter are presented, which show a substantially higher heat flux at the tangency point than is calculated conventionally. This is shown to agree with the analysis of the TPA thermocouple data, thus demonstrating the relevance of the results to large Tokamaks. The cross-field flux measured experimentally is about an order of magnitude higher than that predicted by the theoretical models considered. Spectroscopic observations of the TPA in the visible region are described, which measure the angular dependence of the recycled fluxes and carbon impurity production rate.

1. INTRODUCTION

THE EXPERIMENTS described in this paper were prompted by a number of unresolved questions related to the problem of how the fluxes of particles and energy to and from a surface in a magnetized plasma depend on the angle between that surface and the magnetic field vector. In designing limiters or divertor plates to withstand high powers, it is usually assumed that the heat and particle flux densities along the magnetic field dominate over the cross-field fluxes by orders of magnitude. Hence it is reasonable to assume that the heat and particle fluxes have a $\cos\theta$ dependence, where θ is the angle between the magnetic field and the surface normal. Limiter profiles are employed which use this angular dependence to spread the power over a sufficient area to make the power per unit area of surface tolerable (ULRICKSON, 1986). In ITER and NET (COHEN *et al.*, 1989), where the power densities in the divertor are very large, this philosophy must be taken to an extreme with angles between the total magnetic field vector and the divertor plate surface within 1° of the tangent.

We have developed a new edge diagnostic in an attempt to study the variation of heat and particle fluxes with angle of incidence and compared the results from this diagnostic with infra-red thermography of the moveable limiter on TFTR (DOLL *et*

* Canadian Fusion Fuels Technology Project.
† Institute for Aerospace Studies, University of Toronto, Canada, M3H 5T6.
‡ Plasma Physics Laboratory, Princeton University, Princeton, NJ 08543, U.S.A.

al., 1981). In particular, our investigations have concentrated on the following three areas in which experimental data are required.

1.1. *Impurity production and transport*

A very topical cause for concern is the angular dependence of the sputtering yield. Ion beam experiments have shown that both the deuteron and self-sputtering yields are enhanced by shallow angles of ion impact (ROTH *et al.*, 1989). In Tokamaks, the relationship between surface angle and ion impact angle is complicated by the sheath voltage drop which tends to pull the ions towards the normal. It is a difficult and uncertain process to combine a model for a grazing incidence sheath (CHODURA, 1986) with angular dependence of the yield (DEWALD *et al.*, 1987). There is, however, an indication from JET that the angular dependence of the carbon self-sputtering yield may be the cause of the high Z_{eff} at low densities (STAMP *et al.*, 1989).

Initial results from observations of the spatial distribution of CI spectral emission around the carbon belt limiters on JET provided some indication that the ion flux to the tangency point might be a significant fraction of the parallel flux (PITCHER *et al.*, 1989b). Although it was later found that these results could be largely explained by mean free path effects, it highlighted the potential importance of such an effect. Even if the contribution of such an ion flux to the total were small, it is potentially serious because impurities sputtered from the tangency point would not be effectively screened from the confined plasma by the scrape-off layer (STANGEBY, 1988).

1.2. *Interpretation of Langmuir probes*

In situ Langmuir probes mounted in the r.f. antennae screens, belt limiters and X-point target tiles in JET have provided valuable data on edge parameters (ERENTS *et al.*, 1988; HARBOUR *et al.*, 1989). However, to cope with the high power and long pulses, the probes are designed with a total surface area A_s which significantly exceeds their projected area normal to the magnetic field A_p. The local electron density is obtained from the following equation:

$$n_e = \frac{I_s^+}{A_p e c_s} \tag{1}$$

in which I_s^+ is the probe current at ion saturation and $c_s = \{2eT_e/m_i\}^{0.5}$ is the ion acoustic speed for ions of mass m_i and T_e[eV] is the electron temperature (assumed equal to the ion temperature). The problem is to know what value to assume for A_p. For a Langmuir probe flush with the limiter or divertor plate surface it is conventional to assume that $A_p = A_s \cos\theta$, where A_s is the exposed geometric area of the probe. If the angular dependence were in fact weaker than $\cos\theta$ for small angles this would result in an overestimate of the edge electron density. Preliminary studies on PLT (STANGEBY and MANOS, 1986, private communication) with a probe containing tangential and perpendicular Langmuir and heat flux elements showed perpendicular-to-parallel flux ratios of 10–20%.

The other important parameters derived from the Langmuir probe characteristics are the electron temperature and floating potential V_f. We would expect that at some sufficiently shallow angle the ion and electron flow to the surface would be dominated

by cross-field transport. Since the cross-field transport is anomalous, it is not clear that interpretation of the Langmuir probe characteristics in terms of T_e and V_f is possible. We would like to know at what angle the conventional interpretation breaks down.

1.3. *Heat flux and secondary electron emission*

Given that limiters and divertors are designed assuming a cos θ dependence of the incident power density, it is clearly important to investigate experimentally the limits within which such an assumption is applicable. Secondary electron emission can in theory substantially increase the power flow through the sheath (MATTHEWS *et al.*, 1987) but it is usually assumed in reactor modelling that at the grazing angles required for the power handling, the secondaries will gyrate almost parallel to the surface and so be reabsorbed (CHODURA, 1986).

2. EXPERIMENT

Figure 1(a) shows a schematic diagram of the Tilting Probe Array (TPA). It consists of a 60 mm × 40 mm flat graphite plate which pivots in the range $\theta = 45°$–$100°$ with

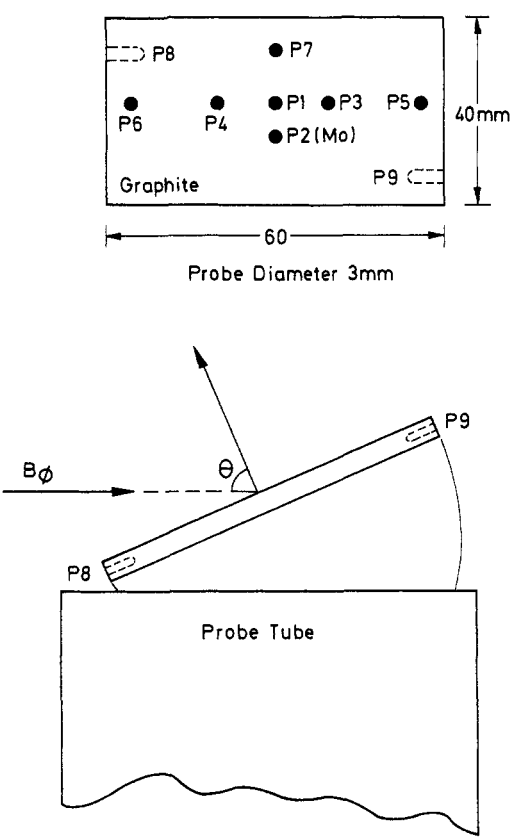

FIG. 1(a).—The Tilting Probe Array—front face (upper), side view (lower).

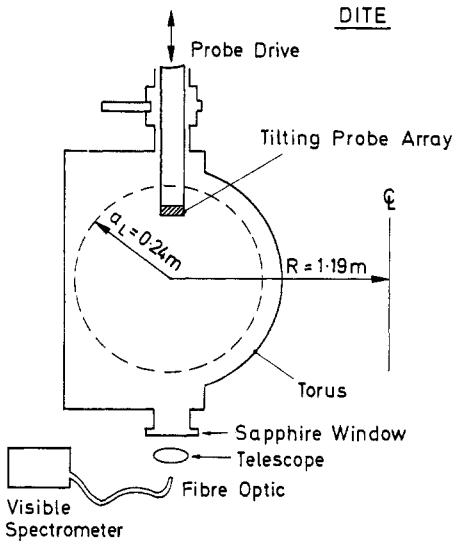

FIG. 1(b).—The Tilting Probe Array is mounted on a top centre port of the DITE torus and is viewed through a window at the bottom.

respect to the toroidal magnetic field. The angle can be changed between shots using a micrometer, to an accuracy considerably better than 1°. The TPA was mounted on the top of the DITE Tokamak, as shown in Fig. 1(b), and levelled to better than 1°. It enters the torus through a port which is located at a major radius of 1190 mm, corresponding to the axis of the outer magnetic flux surface.

Flush with the front surface of the TPA are seven Langmuir probes P1–P7, each of 3 mm diameter, positioned as shown in Fig. 1(a). Each probe is located in a hole of 3.5 mm diameter, giving a clearance of 0.25 mm. Assuming that a maximum of 50% of the flux which enters the annulus between the probe and the clearance hole goes to the probe, the maximum effective probe area would be 17% above its geometric area. This number is kept as small as possible because it is likely to have some angular dependence which is at present impossible to predict.

Our objective in installing an array of probes was to see if there were any edge effects or poloidal variations across the surface. Additional probes P8 and P9 were also fitted in each end of the plate with their centres located 3 mm back from the front face. These probes provide a measure of the Langmuir characteristics at near normal incidence when the front face probes are parallel to the magnetic field.

All probes are made from carbon, except for P2 which is molybdenum. This was intended to investigate whether the different secondary electron emission yields for the two materials influenced the results. Thermocouples are also installed in probes P1 and P2 to give a measure of the energy deposited during each discharge.

Spectroscopic observations of the TPA surface were made from a window on the bottom of the torus. A visible spectrometer fitted with an Optical Multichannel Analyser was focused on the centre of the Tilt Probe and used to make observations in the region of 426.7 and 587.6 nm.

3. RESULTS

The results presented here were all obtained during steady-state conditions in Ohmically heated DITE discharges with a plasma current of 100 kA, toroidal magnetic field of 1.55 T and a line-average density, $\bar{n}_e$, of around 3×10^{19} m^{-3}, with helium as the working gas. The limiter radius was 0.24 m.

3.1. *Current–Voltage characteristics*

Figure 2(a) shows a compilation of Langmuir probe characteristics from P1, for five angles from $\theta = 60°$ to 90°, where the lines have been drawn to guide the eye only. As would be expected, the ion and electron saturation currents, I_s^+ and I_s^-, decrease with the angle to the magnetic field. Figure 2(b) shows a compilation of the results for angles in the range $\theta = 80°$–90°. From this we can see that the ion saturation current I_s^+ falls off more slowly with angle than the electron saturation current I_s^-. For angles within a few degrees of the tangency, $I_s^+ > I_s^-$ and the floating potential shifts to more positive values.

The angular dependence seen on P1 is reproduced on the other six probes in the front surface. Figure 2(c) shows a compilation of probe characteristics from probes P1, P3, P4, P5, P6 and P7 for $\theta = 90°$. The characteristics are almost indistinguishable with the exception of P6, the probe nearest the ion drift side, which collects twice the

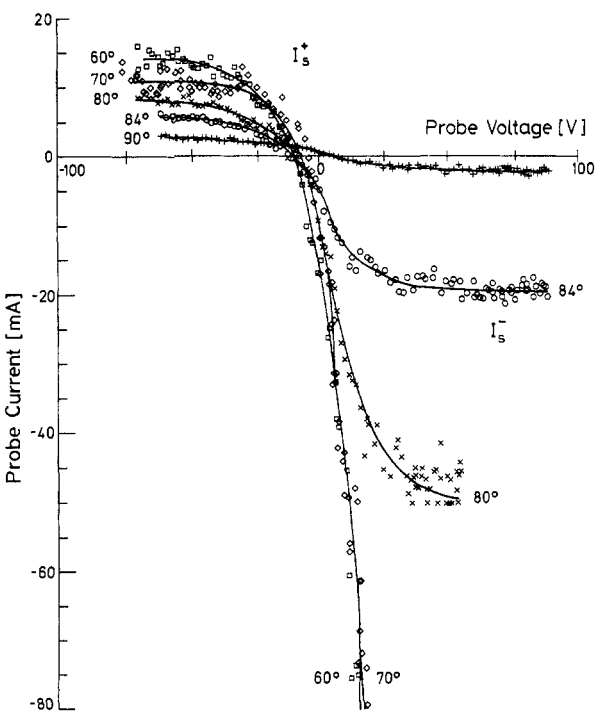

FIG. 2(a).—A compilation of Langmuir probe characteristics from P1 for angles in the range $\theta = 60°$–90°.

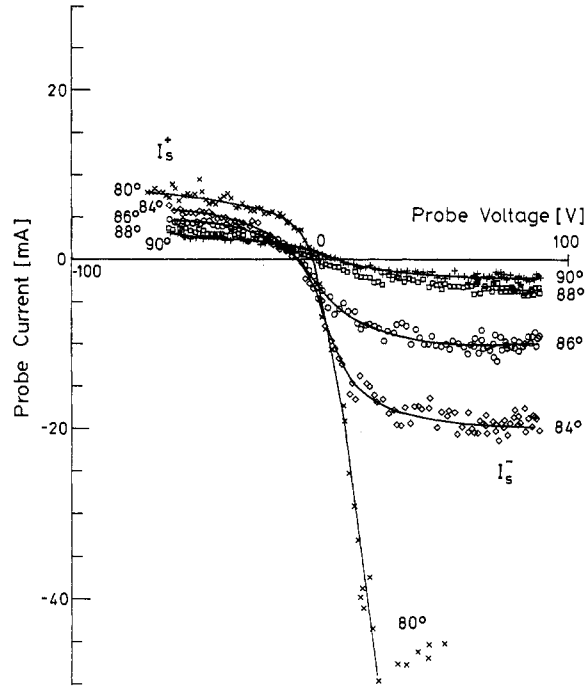

FIG. 2(b).—A compilation of Langmuir probe characteristics from P1 for angles in the range $\theta = 80°$–$90°$.

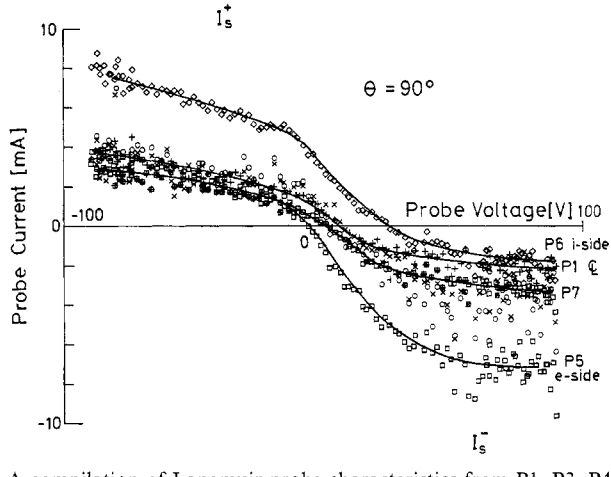

FIG. 2(c).—A compilation of Langmuir probe characteristics from P1, P3, P4, P5, P6 and P7 for $\theta = 90°$. P1+, P3 ○, P4 ×, P5 □, P6 ◇, P7 ⊠.

ion saturation current, and P5 which is on the electron drift side and collects twice the typical electron saturation current.

As the surface is tilted the radii of the probes vary. This has a significant effect for angles $< 80°$ where the radial motion becomes comparable to the e-folding length of the radial profile. Fortunately, since the probes on opposite sides of the tilt probe move in opposite directions it is always possible to interpolate the data to the point of constant radius.

Figures 3(a) and 3(b) show the angular dependence of the ion and electron saturation currents, interpolated to a constant radius. I_s^+ and I_s^- are simply assumed to be the average of the points in the top 10 volts and bottom 10 volts of the scan respectively. The ion saturation current is normalized to the flux at normal incidence so that it can be compared to $\cos\theta$ (solid line). In this series of shots, electron saturation current data were obtained only for $80° < \theta < 100°$ and so the normalization to $\cos\theta$ is carried out at 80°. It can be seen that I_s^+ begins to depart significantly from a $\cos\theta$ dependence for angles within 5° of tangency. Within about 2° of tangency the ion flux is independent of angle at a level equal to 10% of the flux at normal incidence. The electron saturation current, on the other hand, decreases slightly faster than $\cos\theta$ over the measured range except within 2° of tangency. At tangency it is small but finite.

The electron-to-ion saturation current ratio is plotted in Fig. 3(c) over the range 80°–100° for probe P1. It falls below unity within a few degrees of the tangency point. This is also the range of angles for which the floating potential shows a shift in the positive direction.

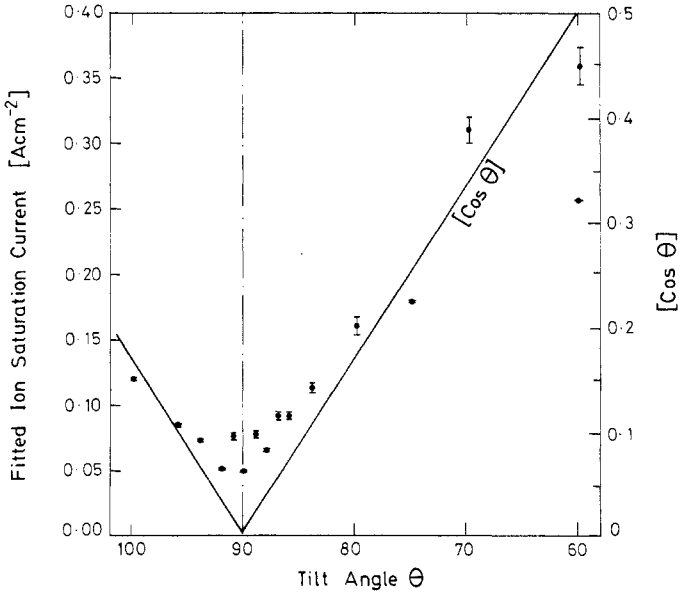

FIG. 3(a).—Angular dependence of the ion saturation current interpolated to constant radius $r = 220$ mm. Typically 5–10 voltage scans were carried out at each angle and the error bars represent standard deviations.

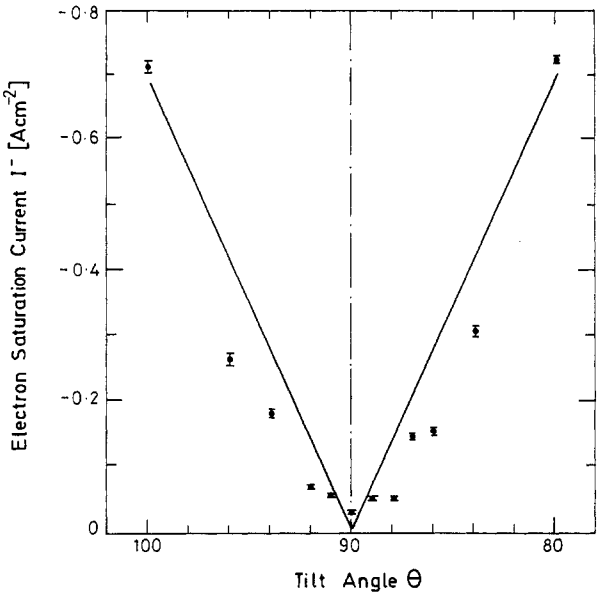

FIG. 3(b).—Angular dependence of the electron saturation current interpolated to constant radius $r = 220$ mm.

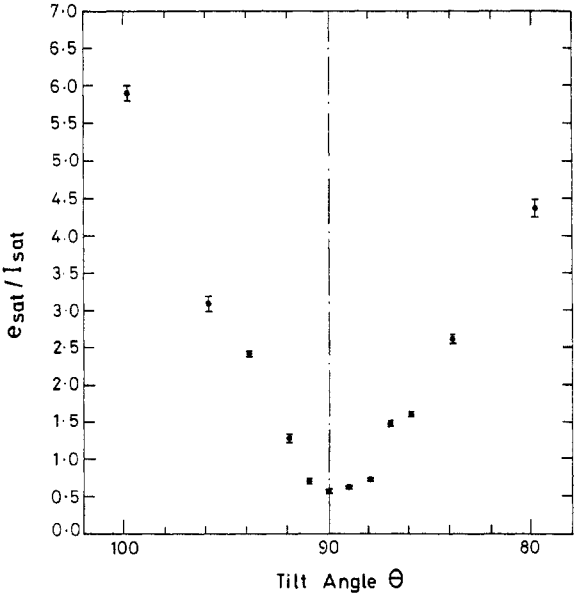

FIG. 3(c).—Angular dependence of the electron-to-ion saturation current ratio interpolated to constant radius $r = 220$ mm.

3.2. *Fitting the Langmuir characteristics*

The standard procedure for extracting useful parameters from single Langmuir probe characteristics is to fit the function:

$$I = I_s^+ \left\{ 1 - e \frac{(V - V_f)}{T_e} \right\} \tag{2}$$

where V is the voltage applied to the probe, I the resulting current, T_e is in electron volts and V_f is the floating potential in volts. The three parameters I_s^+, T_e and V_f are usually optimized using a non-linear least-squares fit to the data. Theoretical arguments about the effect of the magnetic field on the electron flow lead to the conclusion that the data for voltages above V_f should be rejected (STANGEBY, 1982) and there is evidence from JET to support this view (TAGLE *et al.*, 1987). Once the three fitted parameters are obtained the electron density can be derived using equation (1).

To design and interpret Langmuir probes reliably the range of angles over which the analysis of the characteristics is valid must be known. In other words, when is it valid to use the projected area to deduce an electron density and is the fitted electron temperature equal to the real electron temperature in the plasma?

Figure 4 shows examples of fitted Langmuir probe characteristics for angles of 80° and 90°. Provided that we cut off all points above floating potential the fit looks reasonable in both cases. However, the fitted electron temperature at 90° is almost double that for an angle of 80°. This results from the fact that the ion current does not appear to saturate at 90° but shows an almost linear increase with applied voltage. Since we would not expect the actual electron temperature to vary for such a small

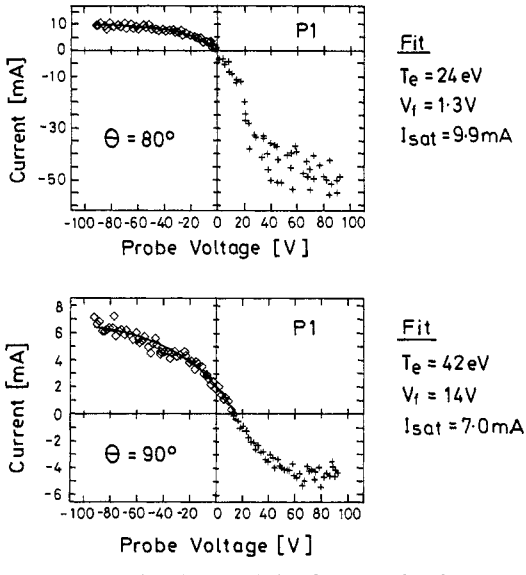

FIG. 4.—Fitted Langmuir probe characteristics from P1 for $\theta = 80°$ (top) and $\theta = 90°$ (bottom). Only the points marked ◇ which are below the floating potential are used to fit the Langmuir probe characteristic.

change in angle, this effect is almost certainly the result of a change in the ion and electron transport to the surface of the Langmuir probe.

In Fig. 5(a), the fitted electron temperature from P1, interpolated to constant radius, is plotted as a function of angle. Although there is some scatter in the fitted electron temperature due to shot-by-shot variations, there is a clear peak in the apparent electron temperature within a few degrees of tangency. Figure 5(b) shows the fitted floating potential from P1 in the range 80°–100°. The positive shift when the magnetic field is at grazing incidence to the surface is quite pronounced.

3.3. *Radial profiles*

With the probe array tilted to the tangency position, a radial profile of the Langmuir probe data was obtained. Figure 6(a) shows the radial behaviour of the ion saturation current density I_s^+/A_s recorded by probes P2, P3, P4, P5 and P7, which are tangential, and probes P8 and P9 which are at normal incidence. The ratio of the two is also plotted and falls from 12 to 5 over the radial range studied. It would be impossible for us to deduce anything about the plasma density from probes P2–P7 since the projected area should be close to zero ($\theta = 90° \pm 1°$). If the $\cos\theta$ rule were to hold true then the current density recorded by P2–P7 would correspond to a probe angle in the range $85.3° > \theta > 78.5°$, which is at least an order of magnitude greater than the probable alignment errors for the system.

In Fig. 6(b) the profiles of electron temperature are plotted. There appears to be no connection between the two profiles. As would be expected, the end probes see a gradual decline of temperature with radius, but the tangential probes measure a much higher electron temperature, independent of radius. It may be concluded that the

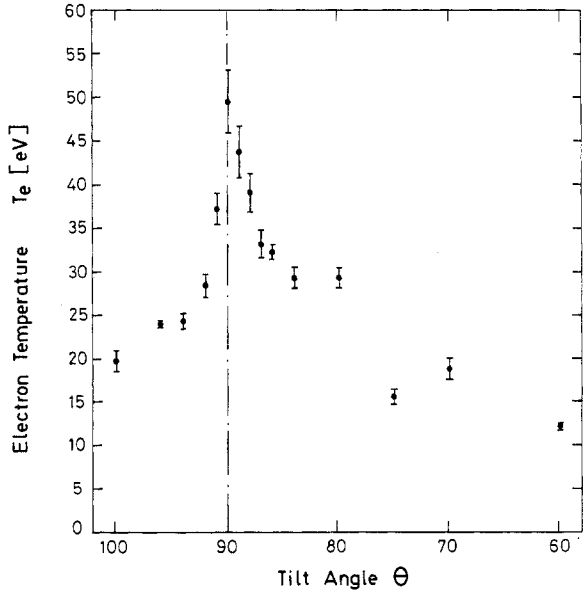

FIG. 5(a).—Fitted electron temperature plotted as a function of surface angle.

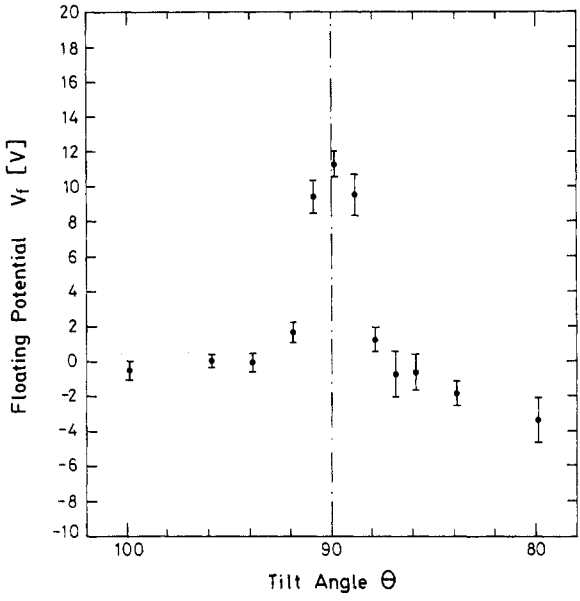

FIG. 5(b).—Fitted floating potential plotted as a function of surface angle.

fitting function (2) is inapplicable in the case of grazing incidence and that the fitted T_e is unrelated to the actual T_e.

3.4. *Spectroscopy*

The abnormal nature of Langmuir probe characteristics for angles close to tangency leads one to ask whether the fitted ion-saturation current is the same as the ion flux to a floating surface. In other words, is the bias voltage applied to the probe causing the ion flow to its surface? To help answer this question, spectroscopic measurements of the HeI (587.6 nm) and CII (426.7 nm) lines have been made as functions of angle using the visible spectrometer system, as shown in Fig. 1(b). The intensities of these lines are relative measurements of the He and C fluxes leaving the probe surface.

In Fig. 7, the intensities for HeI and CII are plotted as functions of angle. The data have been corrected by subtracting the background line emission from a similar shot with the tilting probe array withdrawn. Also plotted on the same scale is the fitted ion saturation current extrapolated to a constant radius. This shows similar behaviour to the HeI and CII light. For these measurements the spectrometer was focused on a spot several centimetres in diameter and the intensity of the HeI should be proportional to the recycled flux at the centre of the graphite plate. The fluence is sufficiently high that it is safe to assume that the surface is saturated and hence that the recycled and incident helium fluxes are equal.

The line emission data were taken during a series of discharges where the front surface of the tilting probe was electrically floating. The HeI has a similar angular dependence to the fitted ion saturation current, indicating that the ion flux to the negatively biased probe is comparable to that incident on a floating surface. When

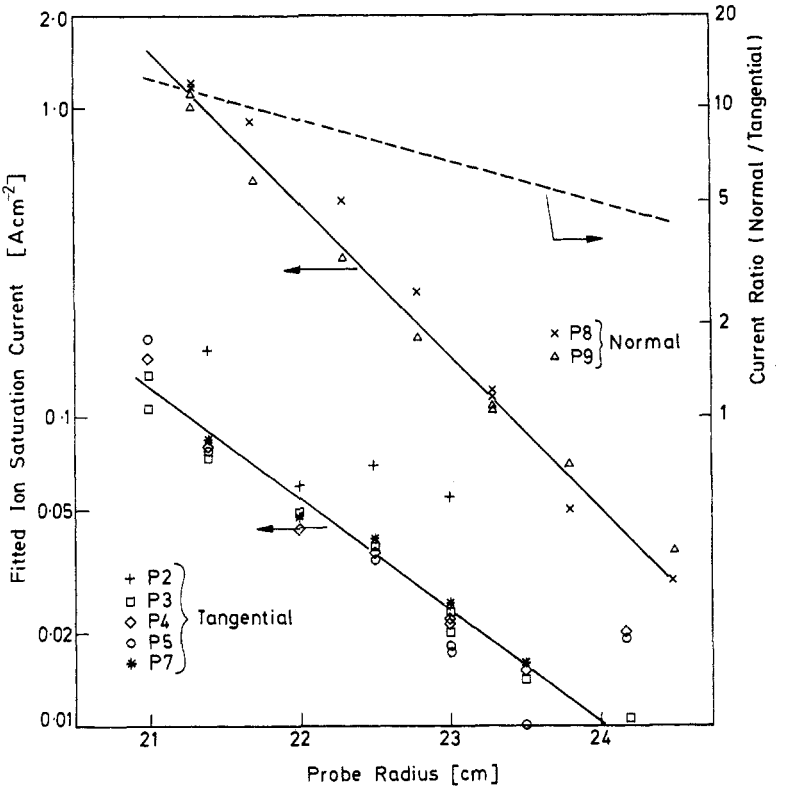

FIG. 6(a).—Radial behavior of fitted ion saturation current from probes normal and tangential to the magnetic field. The ratio of the current to the normal and tangential probes is shown by the dashed line.

the tilt probe surface is at small angles to the magnetic field it is unlikely that there is a significant contribution to the HeI signal from the edges. This is because the sides of the tilting probe array are square and so there is no line of sight for neutrals leaving the side to cross the probe mid-plane. For example, at an angle of 80° a helium neutral leaving the side of the probe would have to travel a distance of 17 cm towards the centre of the plasma, before crossing the sightline of the spectrometer. Since the ionization mean free path is of order a few centimetres, edge effects are unlikely to explain the high level of the HeI signal at tangency. However, we cannot entirely rule out the possibility that CII ions stream along the field into the line of sight or that HeI is observed at the centre of the probe due to charge exchange collisions.

3.5. *Sputtering*

It had been hoped that the tilting probe array would provide information on the angular dependence of the carbon sputtering yield. This can be deduced from the ratio of the HeI to CII line intensities, which are plotted in Fig. 7. This ratio is independent of angle, indicating that there is no angular dependence for the sputtering yield.

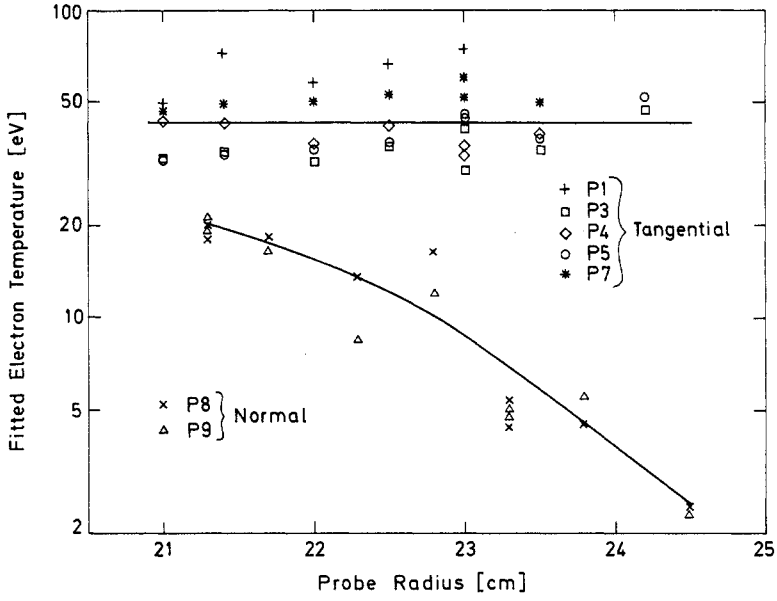

FIG. 6(b).—Radial behaviour of fitted electron temperature from probes normal and tangential to the magnetic field.

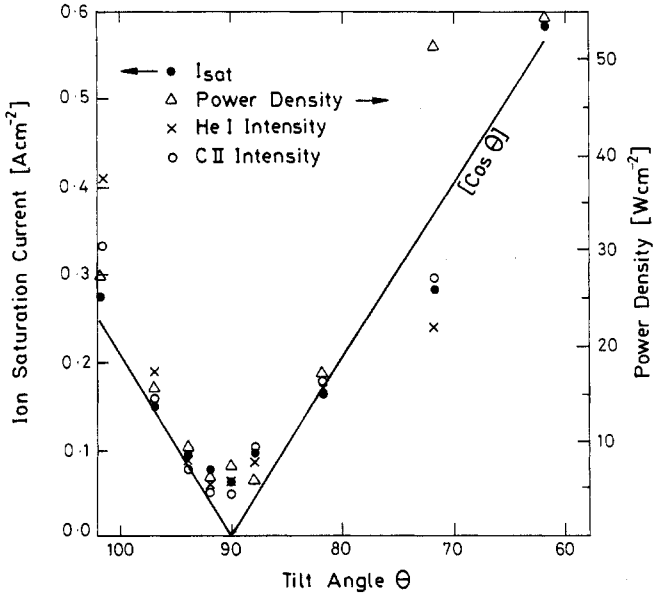

FIG. 7.—Angular dependence of the spectral areas of HeI (587.6 nm) and CII (426.7 nm). Also shown are the fitted ion saturation current and power density from the thermocouple in P1 for the same sequence of discharges.

Following the period when the tilting probe array experiments were carried out, a plasma ion mass spectrometer (PIMS) (MATTHEWS, 1989) was mounted on the same probe drive and routine measurements of the impurity content and charge state distribution in the scrape-off layer were made. At a similar line average density to that employed for the tilting probe work, the results showed that the concentrations of carbon, oxygen and helium in the boundary were: $n_C/n_e \approx n_O/n_e = 7 \pm 2\%$, $n_{He}/n_e = 30 \pm 5\%$. Because the chemical sputtering yield for oxygen on graphite is unity (ROTH, 1984), the nearly equal carbon and oxygen concentrations clearly show that the impurity production is dominated by the presence of oxygen (PITCHER *et al.*, 1989a).

Since any effect due to variations in the physical sputtering yields will be swamped, the spectroscopic measurements give the expected result that the oxygen chemical sputtering yield for graphite is independent of surface angle. This experiment therefore needs to be repeated in a Tokamak where the oxygen concentration is much lower and under conditions of higher edge temperature where the physical sputtering yields should be increased. Such a decrease in oxygen content could be achieved by gettering the torus.

3.6. *Power*

Since it was necessary to leave the probe at floating potential in order to make meaningful power measurements, only a limited data set is available for the angular dependence of the power to the graphite probe P1. The deposited energy is calculated from the temperature rise recorded by the thermocouple embedded in the probe and the mean power is obtained by assuming a pulse length of 0.65 s. In the composite graph of Fig. 7 there are points corresponding to the power density plotted as a function of surface angle. At $\theta = 90°$ there is still a finite flux which is comparable in normalized amplitude to the ion saturation current and the HeI and CII line intensities. This again indicates that there is a finite flux at the tangency point, even to a floating surface, although the deviation from the cos θ dependence is only significant for angles $< 2°$ from tangency.

An even stronger piece of evidence for the anomalous angular dependence of the power to an unbiased surface comes from infra-red thermography of the TFTR moveable limiter. This is essentially a poloidal rail limiter whose tiles are designed to spread the power out over the maximum toroidal extent. Since the tiles curve gently in the toroidal direction there is always a point at which the surface is tangential to the magnetic field. Figure 8 shows the measured surface temperature and compares it with thermal calculations which assume a cos θ dependence of the power to the surface. The model includes the effects of thermal diffusion within the tile but the time scales are too short to fill in the valley at the tangency point. A correct peak-to-valley ratio is obtained from the model only when it is assumed that there is a cross-field power flux to the surface equivalent to $\approx 10\%$ of the parallel flux. This is almost exactly what is required to explain the TPA results. On the other hand, agreement with the power loading of the ALT II limiter on TEXTOR is obtained using a model with a cos θ assumption, without any enhanced cross-field flux (GOEBEL *et al.*, 1989; MCGRATH, 1990, private communication). It is not possible, however, to assess the level of uncertainty in this assumption from the qualitative data presented.

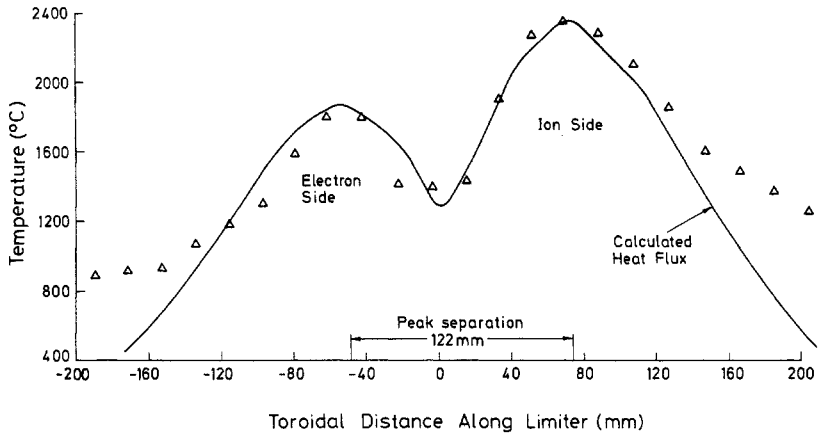

FIG. 8.—Toroidal temperature distribution across a tile on the TFTR moveable limiter at the end of neutral beam injection. Infra-red thermographic measurements are compared with thermal calculations with the assumption that the perpendicular flux = 0.1 × parallel flux.

4. DISCUSSION

4.1. *Limitations for probes*

Our results show that a conventional interpretation of Langmuir probe characteristics becomes invalid for probe angles within 5° of tangency. The fitted electron temperature increases and the floating potential shifts in the positive direction. Also, if the cos θ rule is assumed for the projected area, the calculated electron density can be significantly higher than the true value.

Without a satisfactory theory for grazing incidence probes, correction factors cannot be applied. In addition, the experimental data set is not sufficient to provide empirical correction factors. Flush mounted probes in nearly tangential surfaces should be avoided if the intention is to diagnose the boundary plasma. If in doubt about an existing diagnostic, the best approach would be to look at the electron-to-ion saturation current ratio. If it is near to unity then conventionally fitted data should be regarded as unreliable.

4.2. *Larmor orbits*

Complex kinetic models of the sheath in front of an oblique surface have been developed by CHODURA (1986) which take full account of the ion motion in the magnetic field and the sheath and pre-sheath electric fields. It is, however, implicit in the model that the particle flux densities at the surface have a cos θ dependence and hence the solution for $\theta = 90°$ is singular. The results show only a very weak angular dependence for the measurable quantities such as floating potential and power flux. These calculations can therefore not explain the anomalously high power and particle fluxes close to the tangency point.

Finite ion Larmor radius effects are the most obvious explanation for the observations of non-zero ion fluxes to surfaces tangential to the magnetic field. Figure 9 illustrates schematically how ions within one Larmor radius of the tangential surface will be smeared out over that surface. The Maxwellian averaged ion Larmor radius is given by:

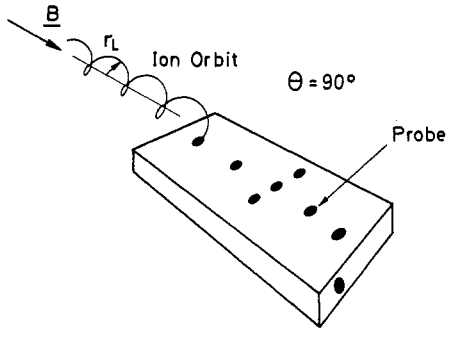

FIG. 9.—Schematic illustration of the finite ion Larmor radius explanation for the ion flux to the tangential face of the probe array.

$$\bar{r}_L = \left(\frac{\pi m_i T_i}{2e}\right)^{0.5} \frac{1}{ZB} = 1.3 \times 10^{-4} \frac{(m_i T_i)^{0.5}}{ZB} \text{ [m]} \tag{3}$$

where T_i is the ion temperature (assumed isotropic), B is the magnetic field strength and M and Z are the atomic mass and charge of the ions. For a helium plasma with the majority of the current carried by He^{2+} ions, a magnetic field of 1.55 T as used in the experiments described here, and assuming an ion temperature in the range $1–3T_e$ (PITTS *et al.*, 1989), gives $\bar{r}_L$ in the range 0.3–0.7 mm.

If ions within one Larmor radius of the surface are spread out uniformly over the distance between the edge and centre of the tilt probe surface (L_s = 30 mm), then the ratio of the flux along the field $\Gamma_{parallel}$ to that normal to the surface Γ_s will be

$$\frac{\Gamma_{parallel}}{\Gamma_s} = \frac{L_s}{\bar{r}_L} = 40–100. \tag{4}$$

When it is also considered that in fact most of these ions would be "scraped off" within a distance of approximately $2\pi\bar{r}_L$ = 2–5 mm of the edge of the tangential surface, it is clear that this argument fails to explain the observed ion flux at the centre of the plate by at least an order of magnitude. It also cannot explain why the ion flux to the tilting probe array is so uniform both in the toroidal and poloidal directions.

4.3. *Surface roughness*

For the above conditions the electron Larmor radius is 7 μm. It is therefore important to know how flat the surface of the tilt probe array is and whether the probe tips are really level with the surface. The maximum deviation of the tilting probe array from perfect surface flatness is 50 μm, which exceeds the electron Larmor radius but is significantly less than an ion Larmor radius. Each probe was also measured with respect to the surrounding surface giving the following results: P1(−32 μm), P2(+55 μm), P3(−2 μm), P4(−5 μm), P5(+7 μm), P6(+5 μm) and P7(+2 μm).

All the deviations in probe depth are comparable to the electron Larmor radius. There is, however, no evidence that the relatively small differences in electron and ion

saturation current between probes are correlated with these imperfections. Even in the case of P1 which is recessed to a depth of four electron Larmor radii there is no significant reduction in the electron flux.

4.4. *Cross-field transport*

An alternative explanation of the high ion flux to the surface at grazing angles is to postulate that it is due to the same anomalous cross-field diffusion process as the radial transport elsewhere in the Tokamak. An estimate of the cross-field diffusion coefficient can be obtained by equating the parallel and perpendicular flux densities in the scrape-off layer as a whole (STANGEBY, 1986) to give the following expression:

$$D_\perp \approx \frac{c_s \lambda_n^2}{L_\parallel} \tag{5}$$

where λ_n is the density decay length and $L_\parallel$ is the connection length between the limiters. With the limiter configuration used in DITE, $L_\parallel = 7.5$ m and from the profiles of Fig. 6 we get $\lambda_n \approx 9$ mm. Assuming also an electron temperature of 15 eV, the value $D_\perp \approx 0.5\ \mathrm{m^2\ s^{-1}}$ is obtained. This is consistent with previous measurements on DITE and is also very similar to results from many other Tokamaks (STANGEBY, 1986; STANGEBY *et al.*, 1988).

The ratio of the parallel to perpendicular fluxes, α, just in front of the tilting probe array will be given by:

$$\alpha = \frac{\Gamma_\parallel}{\Gamma_\perp} \approx \frac{\frac{1}{2} n c_s}{D_\perp \left(\frac{n}{\lambda_n}\right)} = \frac{\lambda_n c_s}{2 D_\perp}. \tag{6}$$

Experimentally we measure a value of $\alpha = 5$–20 which, using the above equation, gives $\lambda_n = 0.3$–1.2 mm which is equivalent to 0.5–$4 r_L$ depending on the ion temperature. This is much smaller than the value of 9 mm measured in the scrape-off layer.

Probe measurements in DITE have shown that the particle transport normal to the field is consistent with the observed electrostatic and density fluctuations (MANTICA *et al.*, 1989). If at tangency the dominant component of the flux is due to fluctuation-driven $\mathbf{E} \times \mathbf{B}$ drifts, the diffusion velocity would be the same for the electrons and ions so that the electron and ion transport to the surface is inherently ambipolar. At angles close to tangency it is observed that the electron and ion saturation currents are nearly equal; see Fig. 2(c). The interpretation of the probe results is complicated by the question of how the biasing process affects the transport of electrons or ions to the probe. However, the available evidence suggests that even with the probe at floating potential the ion flux is comparable to the measured ion saturation current.

The most sophisticated analysis of the flux to a perfectly tangential surface has been carried out by THEILHABER and BIRDSALL (1989) using particle simulation. The model starts with a uniform concentration of electrons and ions, but after one gyro-period ions within one Larmor radius of the surface are absorbed, thus giving rise to a large non-uniform electric field. The $\mathbf{E} \times \mathbf{B}$ drift velocity is strongly sheared, leading

to excitation of the Kelvin–Helmholtz instability and a complex pattern of vortices develops. An effective diffusion coefficient is deduced, given by

$$D_\perp = 0.04 \frac{kT_i}{eB}. \tag{7}$$

For the conditions appropriate to DITE this gives $D_\perp = 0.4$–$1.2\ m^2\ s^{-1}$, which is comparable to the value we have estimated from the profiles. The density scale length derived in the model is $5r_L$, in reasonable agreement with the estimate of 0.5–$4r_L$ calculated earlier in this section. Theilhaber and Birdsall concluded that the flux to the surface at tangency $\Gamma_{\theta=90} = 10^{-2} v_{ti} n_0 \approx 10^{-2} \Gamma_{\theta=0}$, where v_{ti} is the ion thermal velocity and n_0 the ion density far from the surface. Hence, the predictions are qualitatively in agreement with the experiments but the theoretical value of $\Gamma_\perp/\Gamma_\parallel$ is a factor of 10 lower than experiment. Some evidence that the limiter itself does produce fluctuations has been given by HOWLING (1985).

4.5. *Magnetic field structure*

In the TPA experiment on DITE, due to the poloidal field curvature and small uncertainties in the plasma position, there is a finite component of the poloidal field normal to the TPA surface. The total poloidal field of 0.08 T changes the toroidal field angle by 3°. The component of this poloidal field normal to the TPA must be at least an order of magnitude less than this, even given a major positioning error of the probe or plasma. This type of argument therefore cannot explain our results. Other possible explanations for the flux at grazing incidence which have been considered are magnetic islands, banana orbits and magnetic field ripple. Magnetic islands can be rejected on the grounds that the magnetic perturbations involved are far too small, $\sim 0.1\%$, to give any significant change in magnetic field angle. A similar argument can be used to discount magnetic field ripple as an explanation, since in the DITE experiment the variation in angle of incidence over the TPA front face due to the ripple is less than 1°. Banana orbits do not provide the answer either because the motion of the particles is still strongly tied to the toroidal field.

5. CONCLUSIONS

The results presented in this paper from the TPA experiment on DITE and infrared thermography of the moveable limiter on TFTR show that when the magnetic field is at a grazing angle to a limiter surface, the power and particle flux densities do not obey a simple cosine rule. At tangency the ion flux and power flux densities are 5–10% of the flux measured when the magnetic field is at normal incidence to the surface. In contrast, the electron saturation current has a stronger angular dependence at tangency, falling to $< 1\%$ of the value at normal incidence. This means that within a few degrees of tangency the electron saturation current is less than or equal to the ion saturation current. Spectroscopic observations and thermocouple measurements indicate that the ion flux recorded by the Langmuir probes is also representative of the flux to a floating surface.

The electrical measurements have a direct impact on the design and interpretation of Langmuir probes at grazing angles to the magnetic field. A simple $\cos\theta$ interpre-

tation of the results can lead to an overestimate of the electron density. At grazing angles, the floating potential is seen to shift to more positive values and distortion of the Langmuir characteristic occurs, leading to an increase in the fitted electron temperature.

The existence of an anomalous flux to nearly tangential surfaces has important implications for the calculation of the power and particle flux densities to limiters with substantial areas at grazing angles. Further investigations are still required on how such enhancements would affect the edge parameters in the situation where most of the power and particles are deposited on such surfaces, as with toroidal limiters and poloidal divertors. Divertors do differ in one significant respect—the separatrix is far from the divertor plate. The connection length gradually increases as one moves away from the target plate. With limiters the last closed flux surface is defined by the leading edge and hence a discontinuity exists just in front of the limiter itself. A potential beneficial aspect of the results is that small surface misalignments in such structures may not cause as large a non-uniformity in particle and power deposition as might have been thought.

Finite electron and ion Larmor radius effects fail to explain any aspect of the results. When the surface is nearly parallel to the magnetic field the ion flux appears to be enhanced by an increase in the cross-field transport. This may be explained in terms of diffusion down a sharp density gradient of order an ion Larmor radius wide. Kinetic model calculations for the case where the magnetic field is parallel to a surface also produce qualitatively similar results but predict a flux which is about an order of magnitude too low.

The results presented in this paper have important consequences for a range of problems from probe interpretation to reactor design. There is clearly a strong case for further experimental and theoretical work in this area.

Acknowledgements—The authors would like to thank the DITE TEAM for their help and support, and W. DEARING for his mechanical design of the Tilting Probe Array.

REFERENCES

CHODURA R. (1986) in *Physics of Plasma–Wall Interactions* (Edited by D. E. POST and R. BEHRISCH), NATO ASI C Series B Physics, Vol. 131, p. 99. Plenum Press, New York.

COHEN S. A., HARRISON M. F. A., KRASHINNENIKOVS and SUGIHARA M. (1989). Report ITER-IL-PH-13-6-3, July 1989.

DEWALD A. B., BAILEY A. W. and BROOKS J. N. (1987) *Physics Fluids* **30**, 267.

DOLL D. W., ULRICKSON M. and CECCHI J. L. *et al.* (1981) *9th Symp. on Engineering Problems in Fusion Research*, p. 1654. IEEE, New York.

ERENTS S. K., TAGLE J. A. and MCCRACKEN G. M. *et al.* (1988) *Nucl. Fusion* **28**, 1209.

GOEBEL D. M., CONN R. W. and CORBETT W. J. *et al.* (1989) *J. Nucl. Mater.* **162–164**, 115.

HARBOUR P. J., SUMMERS D. D. R., CLEMENT S. *et al.* (1989) *J. Nucl. Mater.* **162–164**, 236.

HOWLING A. A. (1985) Fluctuations in the edge plasma of the TOSCA Tokamak. D.Phil. Thesis, Oxford University.

MANTICA P., CIRANT S., HUGILL J., MATTHEWS G. F., PITTS R. A. and VAYAKIS G. (1989) *Europhysics Conf. Abstracts* Vol. 13B, Part 3, p. 967. Venice, 1989. EPS.

MATTHEWS G. F. (1989) *Plasma Physics Contr. Fusion* **31**(5), 841.

MATTHEWS G. F., MCCRACKEN G. M., SEWELL P., WOODS M. and HOPKINS B. J. (1987) *J. Nucl. Mater.* **145–147**, 225.

PITCHER C. S., FIELDING, S. J. and GOODALL D. H. J. *et al.* (1989a) *Nucl. Fusion* **29**, 1919.

PITCHER C. S., MCCRACKEN G. M., STANGEBY P. C. and SUMMERS D. D. R. (1989b) in *Proc. 15th European Conf. on Controlled Fusion and Plasma Physics*, Vol. 13B, Part 3, p. 879. Venice, 1989. EPS.

PITTS R. A., MCCRACKEN G. M., MATTHEWS G. F. and FIELDING S. J. (1989) in *Proc. 15th European Conf. on Plasma Physics*, Vol. 13B, Part 3, pp. 955–958. Venice, 1989. EPS.
ROTH J. (1984) in *Nuclear Fusion Special Issue: Data Compendium for Plasma Surface Interactions* (Edited by R. A. LANGLEY *et al.*), p. 72.
ROTH J., BOHDANSKY J. and OTTENBERGER W. (1989) *J. Nucl. Mater.* **165**, 193.
STAMP M. F., FORREST M. J., MORGAN P. D. and SUMMERS H. P. (1989) *Europhysics Conf. Abstracts*, Vol. 13B, Part IV, p. 1513. Venice, 1989. EPS.
STANGEBY P. C. (1982) *J. Phys. D.* **15**, 1007.
STANGEBY P. C. (1986) in *Physics of Plasma–Wall Interactions* (Edited by D. E. POST and R. BEHRISCH), NATO ASI Series B Physics, Vol. 131, p. 41. Plenum Press, New York.
STANGEBY P. C. (1988) *Nucl. Fusion* **28**(11), 1945.
STANGEBY P. C., TAGLE J. A., ERENTS S. K. and LOWRY C. (1988) *Plasma Phys. Contr. Fusion* **30**, 1787.
TAGLE J. A., STANGEBY P. C. and ERENTS S. K. (1987) *Plasma Phys. Contr. Fusion* **29**, 297.
THEILHABER K. and BIRDSALL C. K. (1990) *Physics Fluids* **B1**, 2260.
ULRICKSON M. (1986) in *Physics of Plasma–Wall Interactions* (Edited by D. E. POST and R. BEHRISCH), NATO ASI Series B Physics, Vol. 131, p. 855. Plenum Press, New York.